Journal of ELECTRONIC MATERIALS, Vol. 44, No. 4, 2015
DOI: 10.1007/s11664-015-3630-y

Microstructure and Microwave Dielectric Properties of $Ba_{3.75}Nd_{9.5}Ti_{18-z}(Mg_{1/3}Nb_{2/3})_zO_{54}$ Ceramics

HETUO CHEN,[1,2] BIN TANG,[1,3] SHUXIN DUAN,[1] HAN YANG,[1] YINGXIANG LI,[1] HAO LI,[1] and SHUREN ZHANG[1]

1.—State Key Laboratory of Electronic Thin Films and Integrated Devices, University of Electronic Science and Technology of China, Jianshe Road, Chengdu 610054, People's Republic of China. 2.—e-mail: mstuestc@gmail.com. 3.—e-mail: tangbin@uestc.edu.cn

The effects of magnesium and niobium substitution for titanium on the microwave dielectric properties of $Ba_{3.75}Nd_{9.5}Ti_{18-z}(Mg_{1/3}Nb_{2/3})_zO_{54}$ ($0 \le z \le 3$) ceramics were studied. The temperature coefficient of resonant frequency (τ_f) decreased from about +60 ppm/°C to +17 ppm/°C when $z \le 1$. Excellent quality factor (Qf = 7300 GHz) as well as high dielectric constant (ε_r = 80.96) were obtained. For $z \ge 1.5$, $Nd_2(Ti,Mg,Nb)_2O_7$ secondary phase appeared which would obviously influence the microwave dielectric properties. As z varied from 0 to 3, matrix grain size degraded which would obviously deteriorate the microwave dielectric properties by conducting more pores, especially the Qf value. The τ_f value was found to be related to b-site bond valence ($V_{B\text{-}O}$) and unit cell volume (V_m). Average ionic polarizability (α_D) and relative density evidently influenced the dielectric constant.

Key words: Microwave dielectric properties, bond valence, substitution, microstructure

INTRODUCTION

Microwave dielectric ceramics have been widely utilized as components in the filter units of communication systems, such as radar, GPS patch antennas and mobile telephones to select signals.[1–6] The design of new microwave dielectric materials is guided by three criteria updated by Freer and Azough.[2] Materials should have a high relative permittivity to minimize the size of the resonant components, as high as possible Qf, and a near zero temperature coefficient of resonant frequency (τ_f).[2,7]

$Ba_{6-3x}Nd_{8+2x}Ti_{18}O_{54}$-based ceramics, as a series of currently main commercial ceramics, have been attracting attention for their combination of high dielectric constant and high quality factor. However, high positive τ_f (+60 ppm/°C to +150 ppm/°C) has always prohibited their wide utilization.[1,3–6,8–10] Unfortunately, the effect of tetravalent ions substitution at the b-site has been reported to adjust τ_f, and a low dielectric constant and a high dielectric loss, which demand further optimization, were obtained.[11–13] However, this indicated that b-site substitution would be a possible way to modify the τ_f value. Xia et al. reported that divalent ion replacement or pentavalent additives at octahedral site could adjust τ_f while the ceramic system would maintain good dielectric properties.[14–16] Templeton et al. reported the mechanism that divalent cations would restrain Ti reduction to enhance Qf value.[14,17] Moreover, Chen et al. successfully adjusted τ_f towards zero by $(Mg_{1/3}Nb_{2/3})^{4+}$ (coordination number is six, $R^{4+}_{(Mg_{1/3}Nb_{2/3})} = 1/3R^{2+}_{Mg} + 2/3R^{5+}_{Nb}$) substitution in Ti-based perovskite structure ceramics.[7,18,19] So it would be an effective way to adjust τ_f to zero while the ceramic maintained excellent dielectric properties by substituting titanium at the octahedral site with $(Mg_{1/3}Nb_{2/3})^{4+}$. $Ba_{6-3x}Nd_{8+2x}Ti_{18}O_{54}$ (x = 0.75) exhibits relative low τ_f(+60 ppm/°C), therefore minor $(Mg_{1/3}Nb_{2/3})^{4+}$ substitution content would effectively drive τ_f to zero.[1,3,8,9]

In the present work, $Ba_{3.75}Nd_{9.5}Ti_{18-z}(Mg_{1/3}Nb_{2/3})_zO_{54}$ ($0 \le z \le 3$) solid solutions were fabricated and the effects of $(Mg_{1/3}Nb_{2/3})^{4+}$ replacement upon phase constitution as well as microwave dielectric properties were investigated. Secondary phase, bond valence,

(Received October 19, 2014; accepted January 5, 2015; published online February 10, 2015)

grain size, average ionic polarizability and unit cell volume contribution to dielectric properties were also discussed.

EXPERIMENTAL

The ceramics were prepared by the conventional solid-state reaction technique according to the formula of $Ba_{3.75}Nd_{9.5}Ti_{18-z}(Mg_{1/3}Nb_{2/3})_zO_{54}$ with the high-purity starting materials of $BaCO_3$ (Xilong, China), Nb_2O_5 (Ke Long Chemical Reagent, China), $(MgCO_3)_4 \cdot Mg(OH)_2 \cdot 5H_2O$ (Ke Long Chemical Reagent), Nd_2O_3 (Jichang Rare Earth, China) and TiO_2 (Xian Tao Chemical Reagent), with purity ≥99.5%. The mixtures were ball-milled in nylon jars with zirconia balls and distilled water for 12 h. After drying, the powder was calcined at 1000–1100°C for 5 h. Then, the calcined powders were produced with 5 wt.% PVA added in the size of 15 mm in diameter and 6 mm in thickness under a pressure of 220 kg/cm^2. Then, the samples were preheated at 600°C for 2 h to remove the organic binder, and then sintered at 1300–1400°C for 2 h.

The densities of the sintered samples were measured by the Archimedes method. The phase of the sintered samples was identified by x-ray diffraction (XRD) using Cu Kα radiation (Philips x'pert Pro MPD, PANalytical, Netherlands). The surface microstructures of the ceramic were detected by using scanning electron microscopy (SEM). The dielectric characteristics were examined by the Hakki–Coleman dielectric resonator method in the TE_{011} mode using a network analyzer (E5071C; Agilent Technologies, Singapore) at a frequency around 3–5 GHz. The τ_f of the sintered samples at the resonant frequency were determined by the following equation:

$$\tau_f = \frac{f_{t_2} - f_{t_1}}{f_{t_1} \times (t_2 - t_1)} \quad (1)$$

In the equation, f_{t_1} and f_{t_2} are the resonant frequencies at the temperature of t_1 = 25°C and t_2 = 85°C, respectively.

RESULTS AND DISCUSSION

Figure 1 showed x-ray diffraction patterns of $Ba_{3.75}Nd_{9.5}Ti_{18-z}(Mg_{1/3}Nb_{2/3})_zO_{54}$ (z = 0.5–3.0) ceramics sintered at optimum temperature for 2 h. A single $BaNd_2Ti_4O_{12}$ phase of tungsten-bronze structure was obtained for $z \le 1$. This suggested that $Ba_{6-3x}Nd_{8+2x}Ti_{18}O_{54}$ solid solution was formed for a similar ionic radius between $(Mg_{1/3}Nb_{2/3})^{4+}$ (0.0667 nm) and Ti^{4+} (0.0605 nm) site. When $z \ge 1.5$, pyrochlore secondary phase, $Nd_2(Ti,Mg,Nb)_2O_7$ (assigned to JCPDS Card No. 00-042-0002), appeared. As z increased from 1.5 to 3, the main peaks of the second phase became more intense. The results showed that $(Mg_{1/3}Nb_{2/3})^{4+}$ had low solubility in $Ba_{6-3x}Nd_{8+2x}Ti_{18}O_{54}$. The appearance of the second phase indicated that the substitution limit would be $z \le 1$.

The appearance of the second phase originated from the unstable structure always explained by the

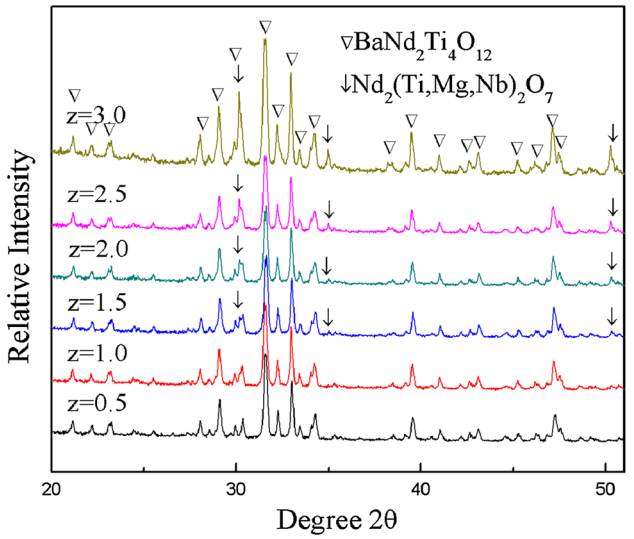

Fig. 1. The XRD patterns of $Ba_{3.75}Nd_{9.5}Ti_{18-z}(Mg_{0.33}Nb_{0.67})_zO_{54}$ ceramics sintered at 1360°C for 2 h as a function of z.

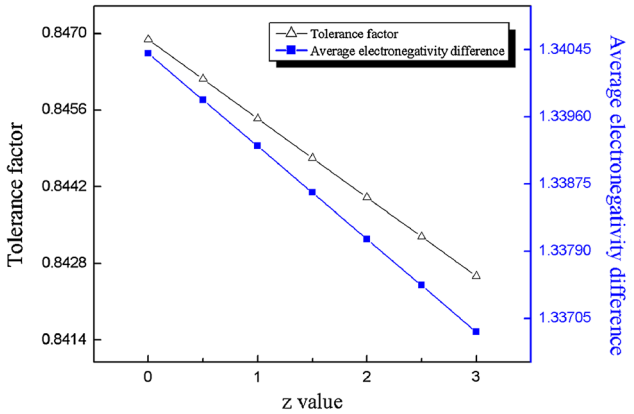

Fig. 2. Tolerance factor t (△) and average electronegativity difference e (□) as functions of z in $Ba_{3.75}Nd_{9.5}Ti_{18-z}(Mg_{0.33}Nb_{0.67})_zO_{54}$ ceramics.

average electronegative difference and tolerance factor of the compositions.[11,12,19] With Pauling's electronegativity scale, the average electronegativity difference could be obtained.[11] According to the theory set by Matveeva et al., the revised equation as follows was taken to calculate the tolerance factor of present compositions:

$$t = \frac{\left(\frac{4}{5} + \frac{x}{5}\right)R_{Nd^{3+}} + \left(\frac{1}{5} - \frac{x}{5}\right)R_{Ba^{2+}} + R_{O^{2-}}}{\sqrt{2}\left(\frac{18-z}{18}R_{Ti^{4+}} + \frac{z}{54}R_{Mg^{2+}} + \frac{z}{27}R_{Nb^{5+}} + R_{O^{2-}}\right)} \quad (2)$$

in which t is the tolerant factor, $R_{Ba^{2+}}$, $R_{Nd^{3+}}$, $R_{Ti^{4+}}$, $R_{Mg^{2+}}$, $R_{Nb^{5+}}$ and $R_{O^{2-}}$, respectively, represent the ionic radii of Ba^{2+}, Nd^{3+}, Ti^{4+}, Mg^{2+}, Nb^{5+} and O^{2-}.[11,12,18,20] Tolerance factors and average electronegativity differences with different z values are illustrated in Fig. 2. Both decreasing tolerance fac-

tor and the average electronegativity difference presaged an unstable structure.[11,12,18]

The relative density of $Ba_{3.75}Nd_{9.5}Ti_{18-z}(Mg_{1/3}Nb_{2/3})_zO_{54}$ (z = 0–3.0) ceramics as a function of z values at different sintering temperatures is illustrated in Fig. 3. For all the compositions, the relative density first increased and reached a maximum density (99%) at 1360°C for $z \le 0.5$. Then, the decreasing relative density for 1380°C appeared, suggesting that 1360°C was the optimum sintering temperature. Meanwhile, the relative density declined with increasing z value and many of them were lower than 95%. Combined with the XRD results, the low relative density was related to the appearance of the secondary phase.

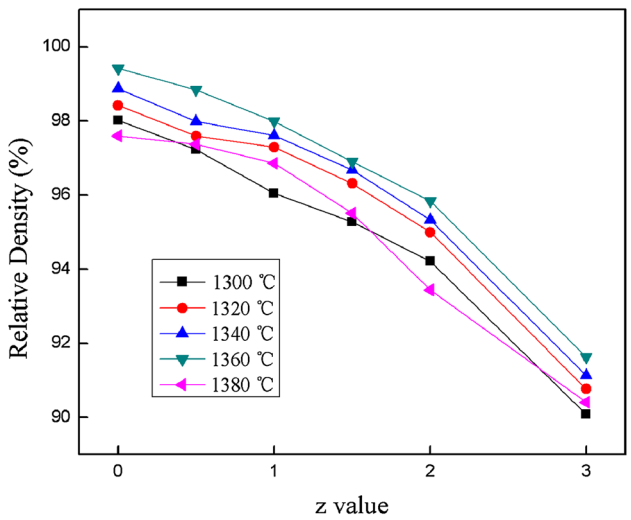

Fig. 3. Relative densities of $Ba_{3.75}Nd_{9.5}Ti_{18-z}(Mg_{0.33}Nb_{0.67})_zO_{54}$ ceramics sintered at different temperatures for 2 h

The microstructures of $Ba_{3.75}Nd_{9.5}Ti_{18-z}(Mg_{1/3}Nb_{2/3})_zO_{54}$ (z = 0–3.0) ceramics sintered at 1360°C are shown in Fig. 4, including typical SEM micrographs and EDS spots A, B and C. The compositions had column grains which have always been observed in $Ba_{6-3x}Nd_{8+2x}Ti_{18}O_{54}$ ceramics.[4,5] Massive grains appeared for $z \ge 1.5$ which was in accordance with XRD results. With increasing z value, grain sizes of these two kinds varied reversely, column grain size degrading from about 10 μm to 4 μm while massive grain size increasing from 2 μm to 8 μm, which indicates that $(Mg_{1/3}Nb_{2/3})^{4+}$ substitution or secondary phase would degrade matrix grain size. Element ratio data of the energy dispersive x-ray analysis (EDS) of spots A, B and C are listed in Table I. Though no Mg was detected at spots A and B, it still supposes the existence of it for its relatively low content. Element ratio results of spots A, B and C confirmed the results that column grains were $BaNd_2Ti_4O_{12}$ and that massive grains were $Nd_2(Ti,Mg,Nb)_2O_7$. However, the element ratio of spot A (in Table I) showing less oxygen numbers than spot B indicates that the substitution prohibited Ti reduction.[21]

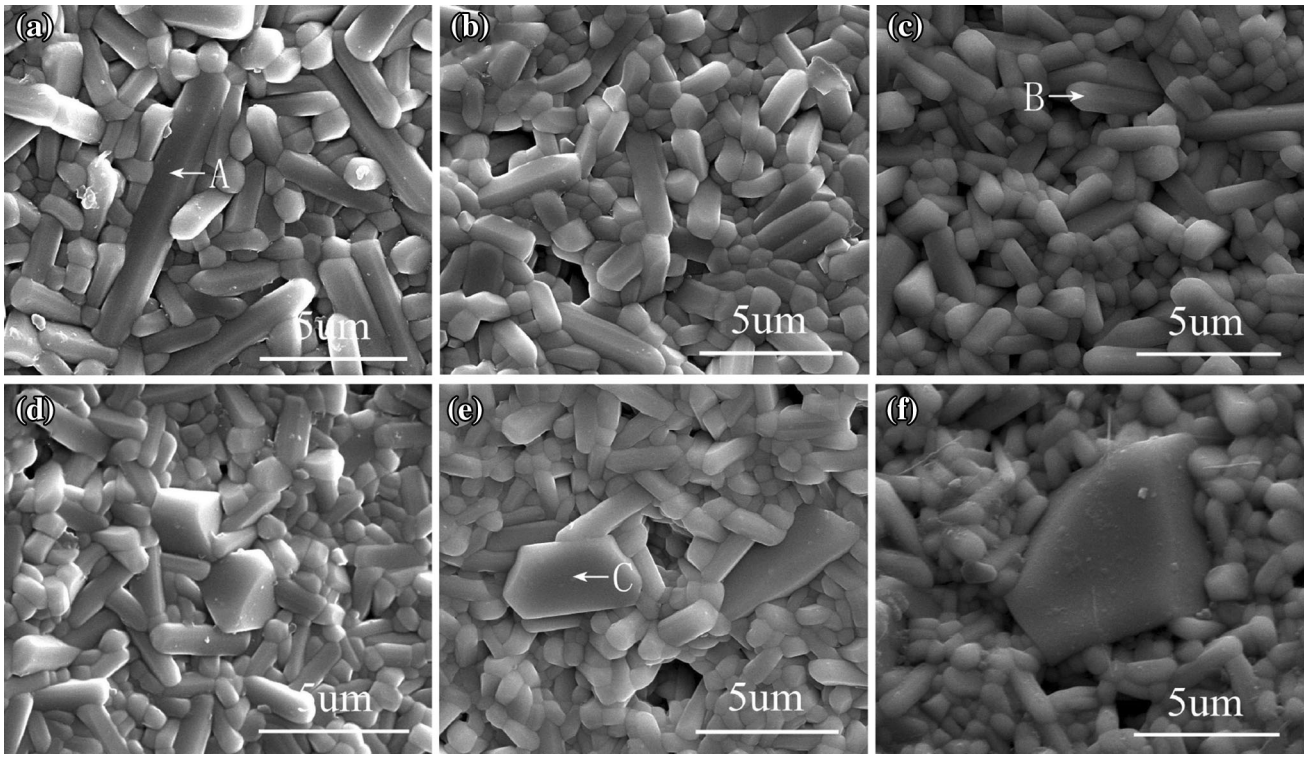

Fig. 4. SEM photographs of magnesium and niobium co-substituted $Ba_{3.75}Nd_{9.5}Ti_{18}O_{54}$ ceramics sintered at 1360°C for 2 h: (a) z = 0.5, (b) z = 1.0, (c) z = 1.5, (d) z = 2.0, (e) z = 2.5, (f) z = 3.0

Figure 5 shows the SEM photographs of $Ba_{3.75}Nd_{9.5}Ti_{17.5}(Mg_{1/3}Nb_{2/3})_{0.5}O_{54}$ sintered at 1300°C, 1340°C, 1360°C and 1380°C, respectively. The average sizes of column grains increased noticeably as the temperature rose from 1300°C to 1360°C, then too high a temperature resulted in abnormal morphology at the surface. The compact microstructure with almost no porosity was obtained at the temperature of 1360°C for $Ba_{3.75}Nd_{9.5}Ti_{17.5}(Mg_{1/3}Nb_{2/3})_{0.5}O_{54}$. Confirmed by XRD results, all images showed no appearance of massive morphology at different temperatures. This implies that the appearance of $Nd_2(Ti,Mg,Nb)_2O_7$ was related not to temperature but to too much substitution. The variation of grain size and porosity illustrated in Fig. 5 is well in accordance with the relative density.

Figure 6 presented the dielectric constant of $Ba_{3.75}Nd_{9.5}Ti_{18-z}(Mg_{1/3}Nb_{2/3})_zO_{54}$ (z = 0.5–3.0) ceramics as a function of sintering temperature. The dielectric constant of samples sintered at optimum

Table 1. EDS data of $Ba_{3.75}Nd_{9.5}Ti_{18-z}(Mg_{0.33}Nb_{0.67})_zO_{54}$ ceramics: A, B and C

	Atom (%)					
Spot	**Ba**	**Nd**	**Ti**	**Mg**	**Nb**	**O**
A	4.66	12.14	22.11	–	–	61.09
B	4.24	11.61	20.23	–	1.02	62.9
C	–	19.41	11.42	4.2	9.07	55.90

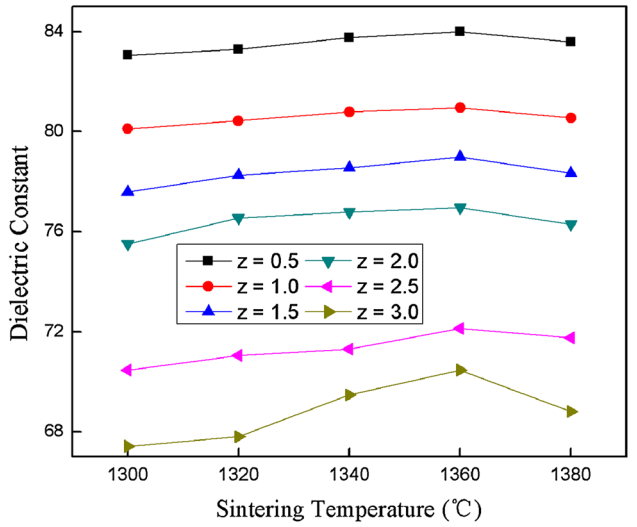

Fig. 6. The dielectric constant of the $Ba_{3.75}Nd_{9.5}Ti_{18-z}(Mg_{1/3}Nb_{2/3})_zO_{54}$ ceramics as a function of sintering temperature

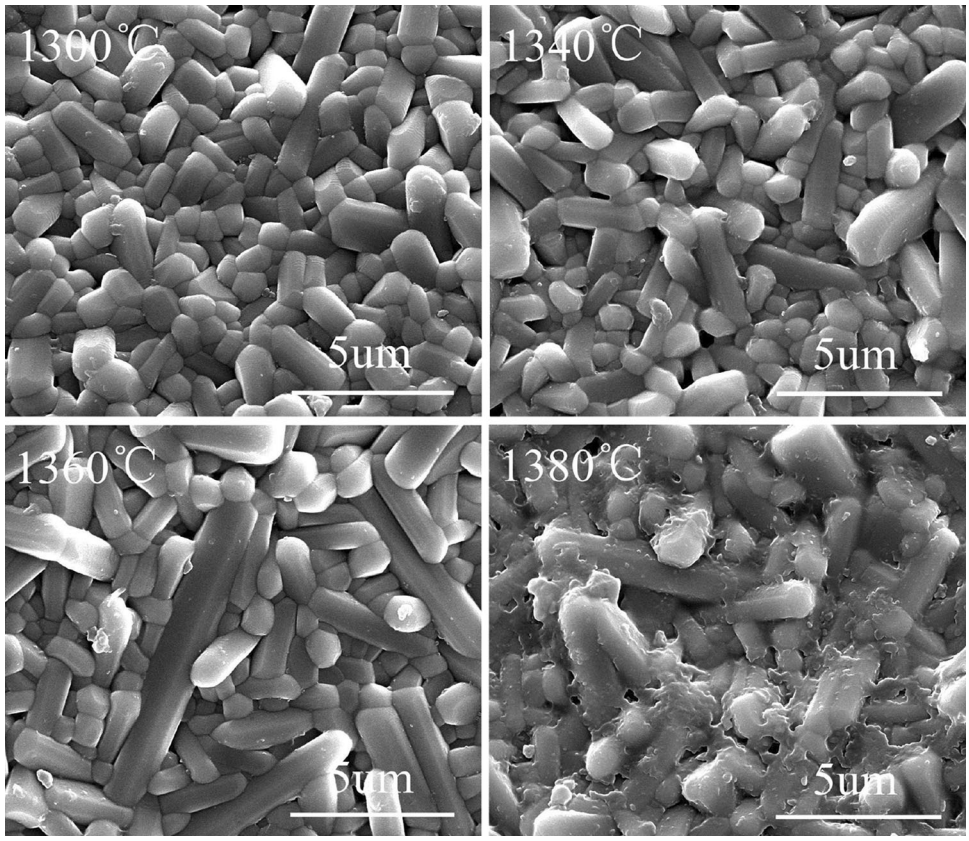

Fig. 5. SEM photographs of $Ba_{3.75}Nd_{9.5}Ti_{17.5}(Mg_{1/3}Nb_{2/3})_{0.5}O_{54}$ ceramics sintered at different temperatures

Table II. Crystal parameters versus composition in $Ba_{3.75}Nd_{9.5}Ti_{18-z}(Mg_{0.33}Nb_{0.67})_zO_{54}$ ceramics

	$z = 0$	$z = 0.5$	$z = 1.0$	$z = 1.5$	$z = 2.0$	$z = 3.0$
a (Å)	22.2386	22.3155	22.9117	22.3811	22.2903	22.3383
b (Å)	12.1637	12.1899	12.1881	12.2317	12.2802	12.2942
c (Å)	3.8383	3.8217	3.8323	3.8382	3.8624	3.8509
V_m (Å^3)	1038.26	1040.80	1041.17	1050.73	1057.21	1057.55
ε_r	87	84	80.96	78.98	76.55	70.47
ε_{rc}	87.54	85.47	84.74	82.77	82.29	77.79
α_D/V_m	0.2307	0.2305	0.2304	0.2303	0.2303	0.2298
R_{B-O}	1.815	1.8156	1.8163	1.8169	1.8176	1.8189
V_{B-O}	2.0901	2.0906	2.0910	2.0914	2.0924	2.0927
η	0.1810	0.1581	0.1376	0.1129	0.1354	0.1809

temperature decreased from 84 to 70.47, which was similar to that of the relative density because the higher density represented lower porosity. Shannon reported that the dielectric constant is directly proportional to the ionic polarizability (α_D) and inversely proportional to the molecular volume (V_m) according to the Clausius–Mosotti equation.[7,15,16,22,23] According to the equation supplied by Lu et al., the corrected dielectric constant (ε_{rc}) can be obtained by modifying the experimental dielectric constant with porosity.[7,16,22,23] The ε_{rc} decreased with an increasing z value and exhibited similar variation as the average ionic polarizability as shown in Table II before $z = 1.5$.[7] For $z \geq 1.5$, the appearance of $Nd_2(Ti,Mg,Nb)_2O_7$ phase ($\varepsilon_r = 36.5$) would also contribute to the declination of dielectric constant.[24] Especially for those results in Fig. 6, there was a sharper decrement for $z = 2.5$ and 3.0 as compared with former samples. The results inferred that the dielectric constant could be controlled by the combination of relative density, average ionic polarizability and secondary phase.

Figure 7 displays the Qf values of $Ba_{3.75}Nd_{9.5}Ti_{18-z}(Mg_{1/3}Nb_{2/3})_zO_{54}$ ($z = 0.5$, 1.0, 1.5, 2.0, 2.5, 3.0) ceramics sintered at optimized temperatures for 2 h. It was obvious that the Qf values of the composition increased greatly to maximum values at 1360°C and then showed a declining trend. Also, the Qf value decreased with z from 0.5 to 3. Usually, many factors, such as pores, second phases, impurities, lattice defects or density, have contributed to the variation of Qf value.[16] In this study, for samples before the appearance of the second phase, the decrease of Qf value was mainly caused by decreasing grain size which has been described above in Fig. 4. Ohsato also reported that intrinsic loss, η, originating from ionic occupancy, played an important role in Qf value:

$$\eta = \frac{\beta}{2\tan\theta} \tag{3}$$

in which β was the full-width at half-maximum of the x-ray powder diffraction peaks and θ was Bragg's angle.[25] The intrinsic loss η (listed in Table II) variation trend was in accordance with Qf

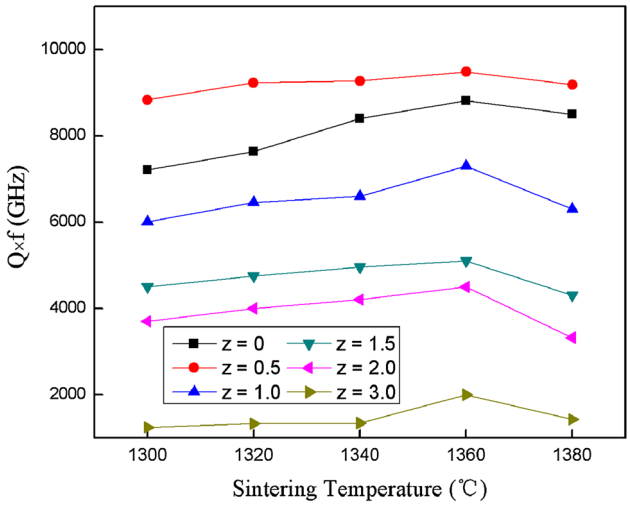

Fig. 7. The Qf value of the $Ba_{3.75}Nd_{9.5}Ti_{18-z}(Mg_{1/3}Nb_{2/3})_zO_{54}$ ceramics as a function of sintering temperature.

value. The result confirmed that the intrinsic loss was related to Qf value. Equally, the EDS data mentioned above implied that the other factor, Ti reduction, influenced the Qf value. The mechanism has been reported by Templeton et al.[21]:

$$2Ti_{Ti}^{x} + O_o^x \rightarrow 2Ti_{Ti}^{'} + V_o^{\cdot\cdot} + \frac{1}{2}O_2 \uparrow \tag{4}$$

Mg substitution prevented the Ti reduction by conducting more oxygen vacancies[17,21]:

$$MgO \xrightarrow{TiO_2} Mg_{Ti}^{''} + O_o^x + V_o^{\cdot\cdot} \tag{5}$$

Yoon et al. reported that Nb addition would modify properties according to the equation[14]:

$$Nb_2O_5 \xrightarrow{TiO_2} 2Nb_{Ti}^{\cdot} + 4O_o^x + \frac{1}{2}O_2 \uparrow + 2e^{'} \tag{6}$$

However, for $z \geq 1.5$, both higher tangent loss of $Nd_2(Ti,Mg,Nb)_2O_7$ phase and decreased matrix grain size did harm to the Qf value of the system.[16,24] To sum up, the Qf value of the system can

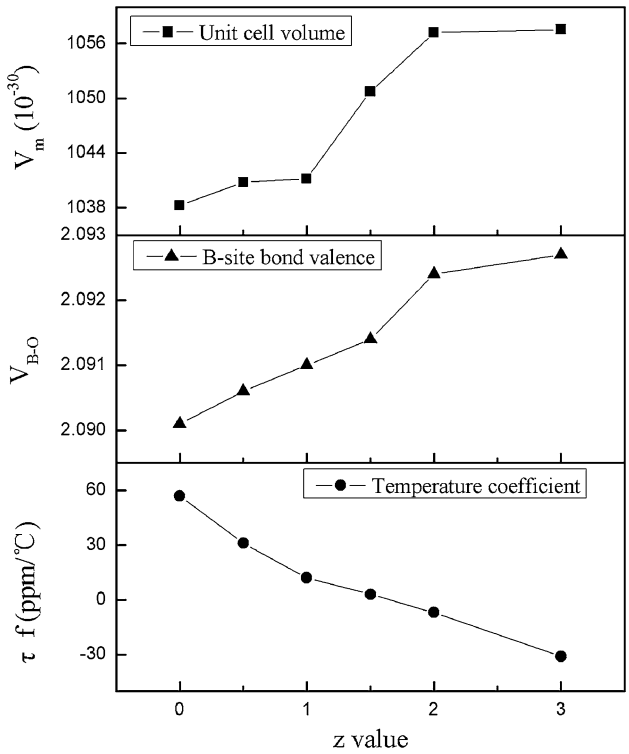

Fig. 8. The τ_f, cell volume and b-site bond valence of the $Ba_{3.75}Nd_{9.5}Ti_{18-z}(Mg_{1/3}Nb_{2/3})_zO_{54}$ ceramics as a function of z value.

be controlled by several factors mentioned above, intrinsic loss η, Ti reduction, and secondary phase.

The variation of τ_f, unit cell volume and b-site bond valence with z is presented in Fig. 8. The negative τ_f of the secondary phase ($\tau_f = -118$ ppm/°C) led to the decrease of τ_f of the system for $z \geq 1.5$.[24] Before the appearance of the second phase, the substitution at Ti site slightly changed the lattice parameters and bond strength represented by bond valence, wch both involving the degree of tilting of the octahedral.[15,16,26] Consequently, they were calculated to evaluate the relationship between them and τ_f. Unit cell volumes were calculated according to XRD data and listed in Table II. B-site substituted bond valence of ceramics was calculated by Eqs. 7 and 8[15,16]:

$$V_i = \sum_j v_{ij} \tag{7}$$

$$v_{ij} = \exp\left(\frac{R_{ij} - d_{ij}}{b'}\right) \tag{8}$$

where R_{ij} was the bond valence parameter, d_{ij} was the length of a bond between atoms i and j, and b' was a universal constant equal to 0.37 Å. The τ_f value variation with increasing z value was reversed with unit cell volume and b-site bond valence. With increasing substitution content of $(Mg_{1/3}Nb_{2/3})^{4+}$ for Ti^{4+}, unit cell volume increased inevitably involving deformed structures, and the result was in accord with Chen et al.[7] The b-site bond strength, evaluated by bond valence, increased. The result was consistent with Huang et al.[16] In conclusion, τ_f was related to the combination of b-site bond valence, unit cell volume and phase composition in $Ba_{3.75}Nd_{9.5}Ti_{18-z}(Mg_{1/3}Nb_{2/3})_zO_{54}$ ($0 \leq z \leq 3$) ceramics.

CONCLUSIONS

Microstructure and microwave dielectric properties of $Ba_{3.75}Nd_{9.5}Ti_{18-z}(Mg_{1/3}Nb_{2/3})_zO_{54}$ ($0 \leq z \leq 3$) system have been investigated in the study. A single phase of $BaNd_2Ti_4O_{12}$ was sustained for $z \leq 1$. B-site bond valence and unit cell volume were related to τ_f. The Qf was greatly controlled by grain size involving pore ratio, Ti^{4+} reduction, and grain size. When $z \geq 1.5$, the pyrochlore second phases of $Nd_2(Ti,Mg,Nb)_2O_7$ appeared and obviously led to the decrease of the Qf value. Relative density, average ionic polarizability and secondary phase together controlled the dielectric constant of the system. Finally, excellent microwave dielectric properties of $\varepsilon_r = 80.96$, $Qf = 7300$ GHz and $\tau_f = +17$ ppm/°C could be obtained when $z = 1$ was sintered at 1360°C for 2 h in air.

ACKNOWLEDGEMENTS

This work is supported by National Natural Science Funds of China (Grant No. 51402039).

REFERENCES

1. M. Sebastian, (Elsevier, Oxford, 2008).
2. R. Freer and F. Azough, *J. Eur. Ceram. Soc.* 89, 1433 (2008).
3. L. Zhang, X. Chen, N. Qin, and X. Liu, *J. Eur. Ceram. Soc.* 27, 3011 (2007).
4. H. Ohsato, T. Ohhashi, S. Nishigaki, T. Okuda, K. Sumiya, and S. Suzuki, *Jpn. J. Appl. Phys.* 32, 4323 (1993).
5. H. Hsiang and T. Chen, *J. Alloy Comp.* 467, 485 (2009).
6. M. Valant and D. Suvorov, *J. Mater. Sci.* 36, 2991 (2001).
7. G. Chen, H. Xu, and C. Yuan, *Ceram. Int.* 39, 4887 (2013).
8. R. Ubic, I. Reaney, W. Lee, J. Samuels, and E. Evangelinos, *Mat. Res. Soc. Symp. Proc.* 453, 495 (1997).
9. P. Setasuwon, R. Freer, F. Azough, and C. Leach, *Adv. Appl. Ceram.* 101, 237 (2002).
10. Y. Fu, C. Liu, C. Lin, and C. Hsieh, *Ceram. Int.* 31, 667 (2005).
11. X. Chen and Y. Li, *J. Am. Ceram. Soc.* 85, 579 (2002).
12. Y. Wu and X. Chen, *Ferroelectr.* 233, 271 (2000).
13. Y. Li, X. Chen, N. Qin, and Y. Zeng, *J. Am. Ceram. Soc.* 88, 481 (2005).
14. K. Yoon, Y. Kim, and E. Kim, *J. Mater. Res.* 10, 2085 (1995).
15. W. Xia, L. Li, L. Ji, P. Zhang, P. Ning, and Q. Liao, *Mater. Lett.* 66, 296 (2012).
16. C. Huang, W. Yang, and P. Yu, *J. Euro. Ceram. Soc.* 34, 277 (2014).
17. A. Templeton, X. Wang, S. Penn, S. Webb, L. Cohen, and N. Alford, *J. Am. Ceram. Soc.* 83, 95 (2000).
18. G. Chen, J. Di, H. Xu, M. Jiang, and C. Yuan, *J. Am. Ceram. Soc.* 95, 1394 (2012).
19. F. Zhao, Z. Yue, Y. Zhang, Z. Gui, and L. Li, *J. Euro. Ceram. Soc.* 25, 3347 (2005).
20. R. Matveeva, M. Varfolomeev, and L. Iluschenko, *Russ. J. Inorg. Chem.* 29, 17 (1984).
21. X. Yao, H. Lin, W. Chen, and L. Luo, *Ceram. Int.* 3, 3011 (2012).
22. R. Shannon, *J. Appl. Phys.* 73, 348 (1993).

23. W. Lei, W. Lu, D. Liu, and J. Zhu, *J. Am. Ceram. Soc.* 92, 105 (2009).
24. T. Junichi, K. Keisuke, and K. Kouhei, *Jpn. J. Appl. Phys.* 32, 4327 (1993).
25. H. Ohsato and J. Euro, *Ceram. Soc.* 21, 2703 (2001).
26. K. Yoon, W. Kim, and E. Kim, *Mater. Sci. Eng.* 99, 112 (2003).